

Recovery of Phosphoric Acid and Calcium Phosphate from Dephosphorization Slag

Shigeru SUGIYAMA^{1*}, Kenta IMANISHI², Naohiro SHIMODA¹, Jhy-Chern LIU³, Hidetoshi SATOU,⁴ and Takaiku YAMAMOTO^{5,6}

¹Department of Applied Chemistry, Graduate School of Technology, Industrial and Social Sciences, Tokushima University, Minamijosanjima, Tokushima-shi, Tokushima 770-8506, Japan

²Department of Chemical Science and Technology, Tokushima University, Minamijosanjima, Tokushima-shi, Tokushima 770-8506, Japan

³Department of Chemical Engineering, National Taiwan University of Science and Technology, 43 Keelung Road, Section 4, Taipei 106, Taiwan

⁴Shimonoseki Mitsui Chemicals, Inc., 7-1-1, Sakomachi, Hikoshima, Shimonoseki-shi, Yamaguchi 750-0092, Japan

⁵Hokusho Co., 6-11-13-319, Fukushima, Fukushima-ku, Osaka-shi, Osaka 553-0003, Japan

⁶Institute for Advanced Study, Kyoto University, Yoshida-Honmachi, Sakyou-ku, Kyoto 606-8501, Japan

Keywords: Dephosphorization Slag, Recovery of Phosphorus, Phosphoric Acid, Calcium Phosphate, Hydroxyapatite

We previously reported that by adding aqueous ammonia to the nitric acid extract of dephosphorization slag, a solid with enhanced concentrations of calcium and phosphorus, could be recovered. The present study shows that a considerable amount of manganese and iron also remains, however, which creates difficulties in directly reusing the recovered solid. The recovered material was again dissolved in nitric acid and the resultant filtrate was passed through a cation exchange resin that mostly removed various cations from the yield of an aqueous phosphoric acid solution. The recovery of phosphoric acid was confirmed via ³¹P NMR. Furthermore, when calcium nitrate was added to this aqueous solution, calcium hydroxyapatite, which was converted to calcium phosphate after the calcination at 1073 K. Phosphoric acid, calcium hydroxyapatite, and calcium phosphate are raw materials that are used to produce various industrial products containing phosphorus, and the suggested process greatly improves the technology for recovering phosphorus-containing materials that are mostly used as fertilizer.

Introduction

Phosphorus is a depleted resource, and the technology for its recovery from various unused waste is being developed worldwide (Ohtake and Tsuneda, 2019). The recycling of phosphorus could be considered an advanced example of the regeneration of other resources. Such technological developments, however, have mostly produced recovered phosphorus that is used as fertilizer. Use of the recovered phosphorus as fertilizer is important, when the low absorption rate of phosphorus by plants is considered, its use as fertilizer tantamount to discarding it in the soil. Furthermore, phosphorus is a raw material for products that ranged from matches to advanced materials such as LEDs, chemical products, and pharmaceuticals (Ohtake *et al.*, 2017). The phosphorus recovered by conventional techniques, however, could not be used in the manufacturing processes of those products. The current phosphorus industry is supported by technologies using phosphate

rock as a raw material. The phosphate rock is composed mainly of calcium phosphates such as calcium phosphate ($\text{Ca}_3(\text{PO}_4)_2$) and calcium hydroxyapatite ($\text{Ca}_{10}(\text{PO}_4)_6(\text{OH})_2$) in particular (Sugiyama *et al.*, 2019; 2020). Phosphoric acid (H_3PO_4), which is the base material for industrial phosphorus-containing products, is produced from the phosphate rock through both wet and dry processes (Al-Fariss *et al.*, 1992; Dorozhkin, 1996; 1997). Therefore, if phosphoric acid and phosphate rock equivalents such as calcium phosphate and calcium hydroxyapatite could be recovered from unused waste, these materials could be directly used in the conventional processes for the current phosphorus industry. The current study shows that it is possible to establish a phosphorus recycling process that advances current resource recycling. Our group previously undertook the recovery of phosphate rock equivalent from chicken manure that was difficult to dispose of and was not being used effectively anywhere in the world. That undertaking clarified that calcium phosphate and calcium hydroxyapatite could be easily recovered by ammonia-treatment of the nitric acid extract from the incineration ash of chicken manure (Sugiyama *et al.*, 2019; 2020) and form composted chicken manure (Sugiyama *et al.*, 2016). We found that chicken manure could be used as a new phosphorus resource. The unused resource that has received the most attention in Japan as a new source of

Received on April 31, 2021, Accepted on June XX, 2021

DOI:10.1252/jcej.21we029

Correspondence concerning this article should be addressed to S.

Sugiyama (E-mail address:sugiyama@tokushima-u.ac.jp)

phosphorus is the dephosphorization slag released during steel processing, since it contains phosphorus that amounts to approximately 80% of the phosphorus imported in the form of phosphate rock by Japan. Most of the slag, however, could not be efficiently used and has been relegated to use as roadbed materials (Kubo *et al.*, 2010). Unfortunately, when the dephosphorization slag was treated in the same manner as chicken manure, a solid with concentrated phosphorus and calcium concentrations was obtained, and considerable amounts of manganese and iron could not be removed (Sugiyama *et al.*, 2014). Therefore, this recovered solid could not be used to directly supply the current phosphorous industry.

The present study was focused on recovering phosphoric acid and calcium phosphate from dephosphorization slag, which was not possible in our previous study (Sugiyama *et al.*, 2014) where the dephosphorization slag was treated using the conventional methods of combining the dissolution with aqueous nitric acid and the subsequent precipitation with aqueous ammonia to recover a solid. This product contained considerable amounts of manganese and iron along with calcium and phosphorus. In the present study, the recovered solid was again dissolved in aqueous nitric acid and the resultant solution was passed through a cation exchange resin to remove unnecessary cations, followed by the formation of phosphoric acid. Then, calcium nitrate was added to this solution in order to ascertain whether calcium phosphate could be produced.

1. Experimental

Dephosphorization slag was supplied from a steel plant in Japan. The composition of the slag was analyzed using X-ray fluorescence (XRF; Supermini 200WD, Rigaku Co.) and the results are described in **Table 1**. The composition of the present slag was similar to that previously used, which was supplied from another steel plant in Japan (Sugiyama *et al.*, 2011; 2014).

Table 1 Composition of dephosphorization slag estimated by XRF spectroscopy

| Composition [%] | | | | | | | |
|-----------------|------|------|------|------|------|------|------|
| Mg | Al | Si | P | Ca | Ti | Mn | Fe |
| 1.69 | 1.39 | 15.8 | 2.72 | 49.5 | 2.37 | 7.89 | 18.6 |

In the present study, dephosphorization slag was treated via a first round of dissolution and precipitation followed by a second round of dissolution and cation removal, and then by a process for the formation of calcium phosphates. All chemicals were purchased from FUJIFILM Wako Pure Chemical Co. and used as supplied. In the first dissolution process, 1.0 g of the dephosphorization slag (particle less than 355 μm) was dissolved in 100 mL 0.5 M HNO_3 at 293 K. This aqueous solution was stirred at 130 rpm for 0.2 h. The resultant

solution was filtered to obtain the residue (solid (I)) and the filtrate (solution (a)). In the precipitation process, aqueous ammonia was added to solution (a) at 200 rpm for 0.5 h to adjust the solution pH = 4. The solution was then let stand for an additional 0.5 h without stirring to allow a precipitate (solid (II)) to form. This aqueous solution was filtered to obtain the precipitate (solid (II)) and the filtrate (solution (b)). In the second dissolution process, solid (II) was dissolved in 100 mL 0.5 M HNO_3 at 293 K, and the resultant solution was then stirred at 200 rpm for 1 h, followed by filtration to obtain the residue (solid (III)) and the filtrate (solution (c)). In the cation removal process, solution (c) was passed through 5.0 g of a strong acid cation exchange resin (PK216LH, Mitsubishi Chemical Co.) in a burette at a flow rate of 2.5 mL/min. Into 50 mL of this resultant solution (solution (d)), 0.236 g of $\text{Ca}(\text{NO}_3)_2 \cdot 4\text{H}_2\text{O}$ was dissolved and the solution was stirred with aqueous ammonia at 200 rpm for 0.5 h to adjust the pH to 7. The resultant solution was let stand for an additional 0.5 h without stirring to allow a precipitate to form. The precipitate was separated via filtration and then dried at 353 K for 24 h. Finally, the dried solid (solid (IV)) was calcined at 1,073 K for 5 h to obtain the final solid (solid (V)). Solids (I)–(V) were analyzed via XRF and/or X-ray diffraction (XRD; SmartLab/RA/INP/DX, Rigaku Co.) spectrometry using $\text{Cu K}\alpha$ radiation (45 kV, 150mA). Solutions (a)–(d) were analyzed using inductively coupled plasma atomic emission spectrometry (ICP-AES, SPS3520UV, SII Nanotechnology Inc.). Furthermore, solution (d) was analyzed using ^{31}P NMR (ECA600, JEOL) at 242.95 MHz of ^{31}P resonance frequency with an external reference of 85% H_3PO_4 solution at 0 ppm at room temperature.

2. Results and Discussion

2.1 First dissolution and precipitation processes

According to our previous study (Sugiyama *et al.*, 2011; 2014), the reaction conditions for the first dissolution and precipitation processes were adjusted to that used in the present study. Under the present conditions, the minimum concentration of nitric acid and the dissolution times were set in the first dissolution process to allow the elution of phosphorus from the dephosphorization slag to reach equilibrium, while the optimal values for solution pH and treatment times for precipitate formation by the addition of aqueous ammonia were used in the precipitation process. As shown in **Table 2**, under the present dissolution conditions, 0.584 and 6.04 mmol/100 mL of phosphorous and calcium, respectively, were dissolved into solution (a) from the slag (1.0 g) in 0.5 M HNO_3 solution (pH = 0.48) in the first dissolution process. The elution of both elements was suitable for a precipitate formation that would approximate the phosphate rock equivalent in the following precipitation process. However, unsuitable

elements such as magnesium, aluminum, manganese and iron were simultaneously detected in amounts of 0.457, 0.185, 0.423 and 0.423 mmol/100 mL, respectively, in solution (a), as reported in our previous study (Sugiyama *et al.*, 2014).

Table 2 Concentration (mmol/100 mL) of each element in solutions (a) and (b) and the corresponding precipitation efficiency (P.E. %)

| Sol. | Mg | Al | P | Ca | Mn | Fe |
|------|-------|-------|-------|------|-------|-------|
| (a) | 0.457 | 0.185 | 0.584 | 6.04 | 0.423 | 0.995 |
| (b) | 0.388 | 0.017 | 0.001 | 5.83 | 0.409 | 0.003 |
| P.E. | 15.1 | 90.9 | 99.9 | 3.6 | 3.5 | 99.7 |

After the first dissolution process, 0.17 g of residue (solid (I)) was recovered, and the compositions of each element in solid (I) are described in **Table 3**. With the exceptions of calcium, phosphorus and silica, the compositions of other elements in the dephosphorization slag (Table 1) were in concentrated forms in the solid (I). However, each element was not selectively separated. In fact, the XRD of solid (I) was not significantly different from that of dephosphorization slag, and the XRD peaks due to Fe_2O_3 (PDF 01-076-8401), CaMgSiO_4 (PDF 00-035-0590), Ca_2SiO_4 (PDF 01-086-0401) and $\alpha\text{-Ca}_3(\text{PO}_4)_2$ (PDF 00-009-0348), were detected, as shown in **Figure 1**.

Table 3 Composition of solid (I), as estimated by XRF spectroscopy

| Composition [%] | | | | | | | |
|-----------------|------|------|------|------|------|------|------|
| Mg | Al | Si | P | Ca | Ti | Mn | Fe |
| 3.50 | 3.84 | 16.0 | 2.10 | 19.9 | 10.3 | 6.98 | 37.3 |

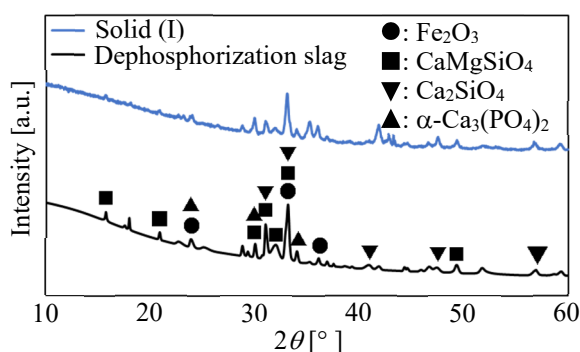


Fig. 1 XRD patterns of dephosphorization slag and solid (I)

To recover the precipitate from solution (a) through the precipitation process, aqueous ammonia was added to solution (a) to obtain 0.363 g of the precipitate (solid (II)) and solution (b) at $\text{pH} = 4$. Table 2 shows the concentration of each element in solution (b) together with the corresponding precipitation efficiency. The precipitation efficiency (P.E.) was calculated using Eq. (1).

$$\text{P.E.}(\%) = (1 - C_b/C_a) \times 100 \quad (1)$$

In Eq. (1), C_a and C_b refer to the concentration (mmol/100 mL) of the corresponding elements in solutions (a) and (b), respectively. During the experiment to determine C_b , the volume of the reference solution changed in the range of 100 ± 3 mL. Therefore, an error with several percent in P.E. could be estimated. As shown in Table 2, the precipitation efficiencies of aluminum, phosphorus and iron were evidently greater, while the corresponding amount of calcium was also precipitated since the concentrations of calcium in solutions (a) and (b) were extremely higher. This indicated that the precipitate (solid (II)) consisted mainly of these four elements. Although the XRD patterns of solid (II) were amorphous, as shown in **Figure 2**, AlPO_4 (PDF 01-073-6179), Fe_2O_3 (PDF 00-001-1053), and $\text{CaFe}_3(\text{PO}_4)_\text{O}$ (PDF 01-078-7784) were detected from solid (II) following calcination at 1,073 K for 5 h, as expected from Table 2. It should be noted that the phosphorus eluted from the dephosphorization slag in the first dissolution process was almost recovered in solid (II). Furthermore, the XRD patterns of solid (II) were completely different from those of the dephosphorization slag, indicating that the second dissolution process of solid (II) may have been influenced by the removal of unwanted elements.

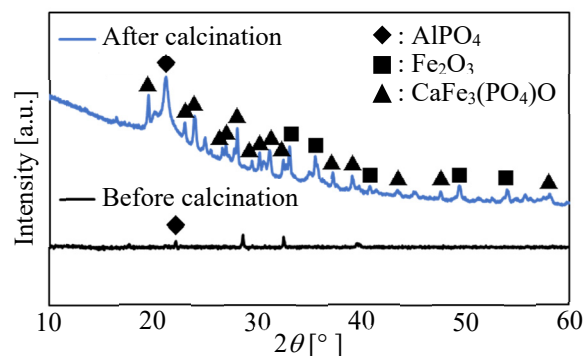


Fig. 2 XRD patterns of solid (II) before and after calcination at 1,073 K for 5 h

2.2 Second dissolution and cation removal processes

To remove unwanted elements from solid (II) through the second dissolution process, 0.363 g of solid (II) was again dissolved in 0.5 M HNO_3 and was separated as the residue (0.118 g; solid (III)) and filtrate (solution (c)). **Table 4** shows the concentration of each element in solid (III) detected using XRF and **Figure 3** shows the XRD patterns of solid (III).

Table 4 Composition of solid (III) estimated by XRF spectroscopy

| Composition [%] | | | | | | | |
|-----------------|------|------|------|------|------|------|------|
| Mg | Al | Si | P | Ca | Ti | Mn | Fe |
| 0.07 | 0.23 | 98.4 | 0.00 | 0.16 | 0.37 | 0.00 | 0.82 |

Table 4 and Figure 3 reveal that solid (III) was amorphous SiO₂ (PDF 01-086-1561) and most of the phosphorus remained in solution (c), which indicated that the silica could be separated from solid (II) could be achieved in the second dissolution process.

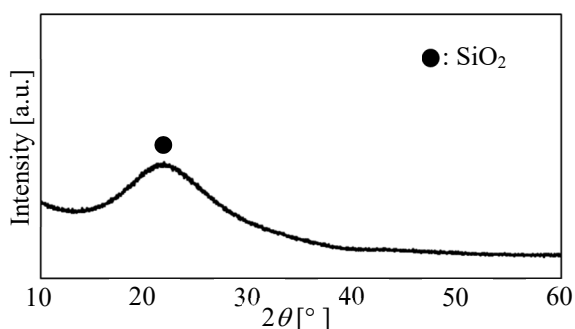


Fig. 3 XRD pattern of solid (III)

Table 5 shows the concentration of each element in solution (c), as detected using ICP-AES. The concentrations of aluminum, phosphorus, and iron in solution (c) (0.147, 0.572, and 0.921 mmol/100 mL, respectively as shown in Table 5) approximated those in solution (a) (0.158, 0.584, and 0.995 mmol/100 mL, respectively, as shown in Table 2). On the other hand, the concentrations of magnesium, calcium, and manganese in solution (c) (0.002, 0.176, and 0.007 mmol/100 mL, respectively, as shown in Table 5) were evidently lower than those in solution (a) (0.457, 6.04, and 0.423 mmol/100 mL, respectively, as shown in Table 2). This indicated that the aluminum, phosphorous, and iron in solution (c) were almost separated from magnesium, calcium, and manganese in solid (III) during the second dissolution process. Therefore, to enrich the concentration of phosphorous in solution (III), the separation of aluminum and iron from solution (c) was conducted in the following cation removal process.

Table 5 Concentration (mmol/100 mL) of each element in solutions (c) and (d)

| Sol. | Mg | Al | P | Ca | Mn | Fe |
|------|-------|-------|-------|-------|-------|-------|
| (c) | 0.002 | 0.147 | 0.572 | 0.176 | 0.007 | 0.921 |
| (d) | 0.000 | 0.001 | 0.478 | 0.004 | 0.001 | 0.005 |

In the cation removal process, solution (c) was passed through a strong acid cation exchange resin to obtain solution (d). The concentrations of each of the elements in solution (d) are also summarized in Table 5. In solution (a) (Table 2), various elements other than phosphorus were present at concentrations higher than that of phosphorus. In solution (d) (Table 5), however, phosphorus was the main component, while the concentrations of other elements were reduced to about 1/100 or lower than the concentration of phosphorus. The above information indicates that it is likely that pure phosphoric acid was formed in solution (d). Therefore, the ³¹P NMR of solution (d) was measured and compared with that of commercially available phosphoric acid

(H₃PO₄). A single ³¹P NMR peak was detected from solution (d) at -0.015 ppm (**Figure 4** (a)) and at 0.000 ppm from the commercially available phosphoric acid (**Figure 4** (b)). Since the chemical shift and splitting pattern due to the ³¹P NMR signal are sensitive to the cation species in the structure (Clayden, 1987; Missong *et al.*, 2016; Zheng *et al.*, 2017), Figure 4 reveals that solution (d) contained fairly pure phosphoric acid.

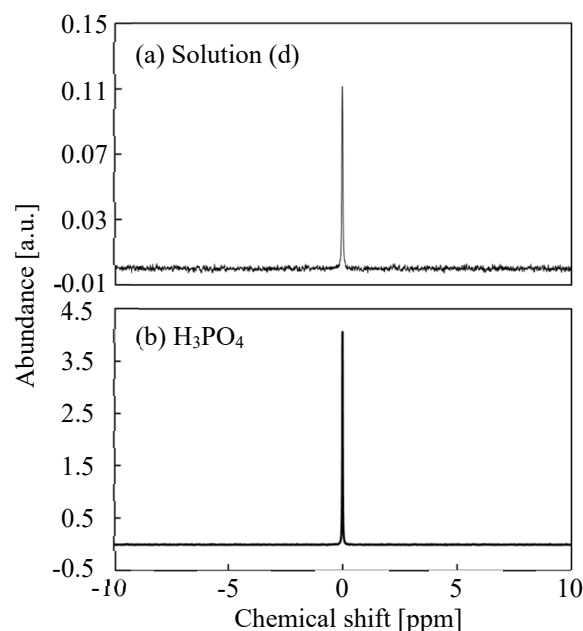


Fig. 4 ³¹P NMR of solution (d) and commercially available H₃PO₄

Table 6 shows the recovery rate of phosphorus in solutions (c) and (d) based on that of solution (a). In the present study, we started the experiment with 100 mL of solution (a) and obtained 98 and 95 mL of solutions (c) and (d), respectively. Therefore, the actual amount of phosphorus in each solution (P in Table 6) was determined from the phosphorus concentration (Conc. P in Table 6) of each solution and from the volume of each solution (V in Table 6). The recovery rate (Recovery in Table 6) was determined by dividing the actual amount of phosphorus recovered by the percentage of phosphorus in solution (a). Based on solution (a), phosphorus was obtained as phosphoric acid with a high recovery rate of 77.8%.

Table 6 Concentrations of phosphorus, solution volumes, and amounts of phosphorus for each solution together with the recovery rate of phosphorus in solution (c) and (d)

| Sol. | Conc. P [mmol/100 mL] | V [mL] | P [mmol] | Recovery [%] |
|------|--------------------------|-----------|-------------|-----------------|
| (a) | 0.584 | 100 | 0.584 | – |
| (c) | 0.572 | 98 | 0.561 | 96.0 |
| (d) | 0.478 | 95 | 0.454 | 77.8 |

2.3 Formation process for calcium phosphates

Since the current phosphorous industry depends on the use of phosphate rock as a raw material, it is important to confirm that phosphate rock equivalents such as calcium phosphate ($\text{Ca}_3(\text{PO}_4)_2$) and calcium hydroxyapatite ($\text{Ca}_{10}(\text{PO}_4)_6(\text{OH})_2$) can be obtained from dephosphorization slag. Furthermore, if calcium phosphate can be obtained by reacting solution (d) with a calcium source, the solution (d) would be confirmed as an aqueous phosphate solution. Therefore, solution (d) was reacted with calcium nitrate, followed by filtration and drying to obtain 0.020 g of a white solid (solid (IV)). The XRD of solid (IV) showed weak peaks probably due to $\text{Ca}_{10}(\text{PO}_4)_6(\text{OH})_2$ (PDF 00-055-0592), while crystallization had not progressed, as shown in **Figure 5**. Thus, solid (IV) was calcined at 1,073 K to obtain solid (V). The XRD pattern of solid (V) matched the reference pattern of $\beta\text{-Ca}_3(\text{PO}_4)_2$ (PDF 01-073-4869). As shown in **Table 7**, solid (V) consisted mainly of calcium and phosphorus, while amounts of aluminum, silica, titanium, manganese, and iron were 1/10 lower contents than that of phosphorus. Phosphate rock consists of calcium phosphate and calcium hydroxyapatite, and this result revealed that phosphate rock equivalent can be obtained from dephosphorization slag. Furthermore, it was confirmed that solution (d) was a relatively high-purity aqueous phosphoric acid.

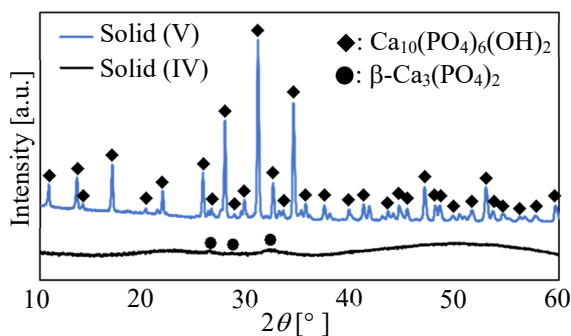


Fig. 5 XRD pattern of solids (IV) and (V)

Table 7 Composition of solid (V) estimated by XRF spectroscopy

| Composition [%] | | | | | | | |
|-----------------|------|------|------|------|------|------|------|
| Mg | Al | Si | P | Ca | Ti | Mn | Fe |
| 0.00 | 0.15 | 2.72 | 27.6 | 64.2 | 2.01 | 0.75 | 2.55 |

Conclusions

The results of this study show that dephosphorization slag treated first by a dissolution process followed by a precipitation process and a second dissolution process, and, ultimately, the process for cation removal process that affords a high-purity aqueous phosphoric acid solution. In the first dissolution process, 1.0 g of dephosphorization slag was added to an aqueous nitric acid solution and most of the slag (0.83 g) was dissolved in the aqueous solution. The constituent

elements in the slag, however, could not be selectively dissolved. In the precipitation process, aqueous ammonia was added to the aqueous solution, and 0.363 g of solid was precipitated. In this process, aluminum, phosphorus, calcium, and iron were concentrated in this solid, and the structure of the solid obtained here was quite different from that of the dephosphorization slag. In the second dissolution process, this solid was again added to an aqueous nitric acid solution. The insoluble residue at this time was amorphous silica, and most of the silicon in the dephosphorization slag could be removed from the aqueous filtrate in this process. In the cation removal process, when the aqueous filtrate obtained in the second dissolution process was passed through a strong acid cation exchange resin, major constituent elements other than phosphorus were removed from the aqueous solution as it passed through the resin. ^{31}P NMR confirmed that the aqueous solution obtained here was a phosphoric acid aqueous solution of relatively high purity. It was also clarified that, when calcium nitrate was added to this aqueous solution, calcium phosphate and calcium hydroxyapatite, which are phosphate rock equivalents, could be obtained. The present study establishes dephosphorization slag as an effective new phosphorus resource that could be used by the current phosphorus industry.

Acknowledgements

This study was conducted as a Collaborative Research Project between Tokushima University and the National Taiwan University of Science and Technology and supported by Steel Foundation for Environmental Protection Technology, for which we are grateful. The authors gratefully acknowledge Dr. Junji Tanaka and Ms Keiko Ideta of Evaluation Center of Materials Properties and Function, Institute for Material Chemistry and Engineering, Kyushu University for measurement and their valuable suggestions on ^{31}P NMR.

Literature Cited

- Al-Fariss, T. E., H. Ö. Özbelge and H. S. H. El-Shall; "Process Technology for Phosphoric Acid Production in Saudi Arabia," *J. King Saud Univ.*, **4**, *Eng. Sci.* (2), 239–255 (1992)
- Clayden, N. J.; "Solid-state nuclear magnetic resonance spectroscopic study of γ -zirconium phosphate" *J. Chem. Soc. Dalton Trans.*, 1877-1881 (1987)
- Dorozhkin, S. V.; "Fundamentals of the Wet-Process Phosphoric Acid Production. 1. Kinetics and Mechanism of the Phosphate Rock Dissolution," *Ind. Eng. Chem. Res.*, **35**, 4328–4335 (1996)
- Dorozhkin, S. V.; "Fundamentals of the Wet-Process Phosphoric Acid Production. 2. Kinetics and Mechanism of $\text{CaSO}_4 \cdot 0.5\text{H}_2\text{O}$ Surface Crystallization and Coating Formation," *Ind. Eng. Chem. Res.*, **36**, 467–473 (1997)
- Kubo, H., K. Matsubae-Yokoyama and T. Nagasaka; "Magnetic Separation of Phosphorus Enriched Phase from Multiphase Dephosphorization Slag," *ISIJ Int.*, **50**, 59–64 (2010)
- Missong, A., R. Bol, S. Willbold, J. Siemens and E. Klumpp; "Phosphorus Forms in Forest Soil Colloids as Revealed by Liquid-State ^{31}P -NMR," *J. Plant Nutr. Soil Sci.*, **179**, 159-167 (2016)

- Ohtake, H., S. Onodera, A. Kuroda, K. Satake, S. Sugiyama, Y. Taketani, M. Hashimoto, S. Mishima and T. Murakami, eds.; Encyclopedia of Phosphorus, Asakura Publishing, Tokyo, Japan (2017)
- Ohtake, H. and S. Tsuneda, eds.; Phosphorus Recovery and Recycling, Springer, Singapore (2019)
- Sugiyama, S., D. Ioka, T. Hayashi, M. Noguchi, K. Nakagawa, K.-I. Sotowa and K. Takashima; "Recovery of phosphate from Unused Resources," *Phosphorus Res. Bull.*, **25**, 18–22 (2011)
- Sugiyama, S., I. Shinomiya, R. Kitora, K. Nakagawa and M. Katoh; "Recovery and Enrichment of Phosphorus from the Nitric Acid Extract of Dephosphorization Slag," *J. Chem. Eng. Jpn.*, **47**, 483–487 (2014)
- Sugiyama, S., R. Kitora, H. Kinoshita, K. Nakagawa, M. Katoh and K. Nakasaka; "Recovery of Calcium Phosphates from Composted Chicken Manure," *J. Chem. Eng. Jpn.*, **49**, 224–228 (2016)
- Sugiyama, S., K. Wakisaka, K. Imanishi, M. Kurashina, N. Shimoda, M. Katoh and J.-C. Liu; "Recovery of Phosphate Rock Equivalents from Incineration Ash of Chicken Manure by Elution-precipitation Treatment," *J. Chem. Eng. Jpn.*, **52**, 778–782 (2019)
- Sugiyama, S., E.-H. Liu, K. Imanishi, N. Shimoda, M. Katoh and J.-C. Liu; "Dependence of Phosphorus Recovery on Acid Type during Dissolution-Precipitation Treatment of Incineration Ash of Chicken Manure," *J. Chem. Eng. Jpn.*, **53**, 667–674 (2020)
- Zheng, A., S.-B. Liu and F. Deng; "³¹P NMR Chemical Shifts of Phosphorus Probes as Reliable and Practical Acidity Scales for Solid and Liquid Catalysts," *Chem. Rev.* **117**, 12475-12531 (2017)